

Direct Measurement of the Pseudoscalar Decay Constant f_{D^+}

M. Ablikim¹, J. Z. Bai¹, Y. Ban¹¹, J. G. Bian¹, X. Cai¹, J. F. Chang¹, H. F. Chen¹⁶, H. S. Chen¹, H. X. Chen¹, J. C. Chen¹, Jin Chen¹, Jun Chen⁷, M. L. Chen¹, Y. B. Chen¹, S. P. Chi², Y. P. Chu¹, X. Z. Cui¹, H. L. Dai¹, Y. S. Dai¹⁸, Z. Y. Deng¹, L. Y. Dong^{1a}, Q. F. Dong¹⁵, S. X. Du¹, Z. Z. Du¹, J. Fang¹, S. S. Fang², C. D. Fu¹, H. Y. Fu¹, C. S. Gao¹, Y. N. Gao¹⁵, M. Y. Gong¹, W. X. Gong¹, S. D. Gu¹, Y. N. Guo¹, Y. Q. Guo¹, K. L. He¹, M. He¹², X. He¹, Y. K. Heng¹, H. M. Hu¹, T. Hu¹, X. P. Huang¹, X. T. Huang¹², X. B. Ji¹, C. H. Jiang¹, X. S. Jiang¹, D. P. Jin¹, S. Jin¹, Y. Jin¹, Yi Jin¹, Y. F. Lai¹, F. Li¹, G. Li², H. H. Li¹, J. Li¹, J. C. Li¹, Q. J. Li¹, R. Y. Li¹, S. M. Li¹, W. D. Li¹, W. G. Li¹, X. L. Li⁸, X. Q. Li¹⁰, Y. L. Li⁴, Y. F. Liang¹⁴, H. B. Liao⁶, C. X. Liu¹, F. Liu⁶, Fang Liu¹⁶, H. H. Liu¹, H. M. Liu¹, J. Liu¹¹, J. B. Liu¹, J. P. Liu¹⁷, R. G. Liu¹, Z. A. Liu¹, Z. X. Liu¹, F. Lu¹, G. R. Lu⁵, H. J. Lu¹⁶, J. G. Lu¹, C. L. Luo⁹, L. X. Luo⁴, X. L. Luo¹, F. C. Ma⁸, H. L. Ma¹, J. M. Ma¹, L. L. Ma¹, Q. M. Ma¹, X. B. Ma⁵, X. Y. Ma¹, Z. P. Mao¹, X. H. Mo¹, J. Nie¹, Z. D. Nie¹, H. P. Peng¹⁶, N. D. Qi¹, C. D. Qian¹³, H. Qin⁹, J. F. Qiu¹, Z. Y. Ren¹, G. Rong¹, L. Y. Shan¹, L. Shang¹, D. L. Shen¹, X. Y. Shen¹, H. Y. Sheng¹, F. Shi¹, X. Shi^{11c}, H. S. Sun¹, J. F. Sun¹, S. S. Sun¹, Y. Z. Sun¹, Z. J. Sun¹, X. Tang¹, N. Tao¹⁶, Y. R. Tian¹⁵, G. L. Tong¹, D. Y. Wang¹, J. Z. Wang¹, K. Wang¹⁶, L. Wang¹, L. S. Wang¹, M. Wang¹, P. Wang¹, P. L. Wang¹, S. Z. Wang¹, W. F. Wang^{1d}, Y. F. Wang¹, Z. Wang¹, Z. Y. Wang¹, Zhe Wang¹, Zheng Wang², C. L. Wei¹, D. H. Wei¹, N. Wu¹, Y. M. Wu¹, X. M. Xia¹, X. X. Xie¹, B. Xin^{8b}, G. F. Xu¹, H. Xu¹, S. T. Xue¹, M. L. Yan¹⁶, F. Yang¹⁰, H. X. Yang¹, J. Yang¹⁶, Y. X. Yang³, M. Ye¹, M. H. Ye², Y. X. Ye¹⁶, L. H. Yi⁷, Z. Y. Yi¹, C. S. Yu¹, G. W. Yu¹, C. Z. Yuan¹, J. M. Yuan¹, Y. Yuan¹, S. L. Zang¹, Y. Zeng⁷, Yu Zeng¹, B. X. Zhang¹, B. Y. Zhang¹, C. C. Zhang¹, D. H. Zhang¹, H. Y. Zhang¹, J. Zhang¹, J. W. Zhang¹, J. Y. Zhang¹, Q. J. Zhang¹, S. Q. Zhang¹, X. M. Zhang¹, X. Y. Zhang¹², Y. Y. Zhang¹, Yiyun Zhang¹⁴, Z. P. Zhang¹⁶, Z. Q. Zhang⁵, D. X. Zhao¹, J. B. Zhao¹, J. W. Zhao¹, M. G. Zhao¹⁰, P. P. Zhao¹, W. R. Zhao¹, X. J. Zhao¹, Y. B. Zhao¹, H. Q. Zheng¹¹, J. P. Zheng¹, L. S. Zheng¹, Z. P. Zheng¹, X. C. Zhong¹, B. Q. Zhou¹, G. M. Zhou¹, L. Zhou¹, N. F. Zhou¹, K. J. Zhu¹, Q. M. Zhu¹, Y. C. Zhu¹, Y. S. Zhu¹, Yingchun Zhu^{1e}, Z. A. Zhu¹, B. A. Zhuang¹, X. A. Zhuang¹, B. S. Zou¹

(BES Collaboration)

¹ Institute of High Energy Physics, Beijing 100049, People's Republic of China

² China Center for Advanced Science and Technology, Beijing 100080, People's Republic of China

³ Guangxi Normal University, Guilin 541004, People's Republic of China

⁴ Guangxi University, Nanning 530004, People's Republic of China

⁵ Henan Normal University, Xinxiang 453002, People's Republic of China

⁶ Huazhong Normal University, Wuhan 430079, People's Republic of China

⁷ Hunan University, Changsha 410082, People's Republic of China

⁸ Liaoning University, Shenyang 110036, People's Republic of China

⁹ Nanjing Normal University, Nanjing 210097, People's Republic of China

¹⁰ Nankai University, Tianjin 300071, People's Republic of China

¹¹ Peking University, Beijing 100871, People's Republic of China

¹² Shandong University, Jinan 250100, People's Republic of China

¹³ Shanghai Jiaotong University, Shanghai 200030, People's Republic of China

¹⁴ Sichuan University, Chengdu 610064, People's Republic of China

¹⁵ Tsinghua University, Beijing 100084, People's Republic of China

¹⁶ University of Science and Technology of China, Hefei 230026, People's Republic of China

¹⁷ Wuhan University, Wuhan 430072, People's Republic of China

¹⁸ Zhejiang University, Hangzhou 310028, People's Republic of China

^a Current address: Iowa State University, Ames, IA 50011-3160, USA.

^b Current address: Purdue University, West Lafayette, IN 47907, USA.

^c Current address: Cornell University, Ithaca, NY 14853, USA.

^d Current address: Laboratoire de l'Accélérateur Linéaire, F-91898 Orsay, France.

^e Current address: DESY, D-22607, Hamburg, Germany.

The absolute branching fraction for the decay $D^+ \rightarrow \mu^+ \nu$ has been directly measured based on a data sample of about 33 pb^{-1} collected around $\sqrt{s} = 3.773 \text{ GeV}$ with the BES-II detector at the BEPC collider. A total of $5321 \pm 149 \pm 160$ D^- mesons are reconstructed in nine hadronic decay modes. In the system recoiling against these singly tagged D^- mesons, 2.67 ± 1.74 purely leptonic decay events of $D^+ \rightarrow \mu^+ \nu_\mu$ are observed. Those yield the branching fraction of $BF(D^+ \rightarrow \mu^+ \nu_\mu) = (0.122^{+0.111}_{-0.053} \pm 0.010)\%$, and a corresponding value of the pseudoscalar decay constant $f_{D^+} = (371^{+129}_{-119} \pm 25) \text{ MeV}$.

son. The virtual W^+ boson is produced in the annihilation of the c and \bar{d} quarks. The decay rate of this process is determined by the wavefunction overlap of the two quarks at the origin, and is parametrized by the D^+ decay constant, f_{D^+} . Fig. 1 shows the decay diagram for the Cabibbo-suppressed purely leptonic decay of the D^+ meson. The decay width of the $D^+ \rightarrow l^+ \nu_l$ is given by the formula [1]

$$\Gamma(D^+ \rightarrow l^+ \nu_l) = \frac{G_F^2 f_{D^+}^2}{8\pi} |V_{cd}|^2 m_l^2 m_{D^+} \left(1 - \frac{m_l^2}{m_{D^+}^2}\right)^2, \quad (1)$$

where G_F is the Fermi coupling constant, V_{cd} is the $c \rightarrow d$ Cabibbo-Kobayashi-Maskawa (CKM) matrix element [2], m_l is the mass of the lepton, and m_{D^+} is the mass of the D^+ meson.

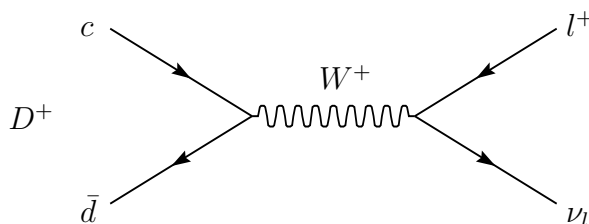


FIG. 1: The decay diagram for $D^+ \rightarrow l^+ \nu_l$.

f_{D^+} is an important parameter. However, it is difficult to measure f_{D^+} due to the fact that the $D^+ \rightarrow l^+ \nu_l$ is a Cabibbo-suppressed decay process. There are some theoretical calculations to estimate the value of f_{D^+} . Although predictions for f_{D^+} vary significantly from 90 to 360 MeV [3], the predictions for the ratios $f_{D^+} : f_{D_S^+} : f_B$ are more reliable, where $f_{D_S^+}$ and f_B are the decay constants for the D_S^+ and the B mesons, respectively. The meson decay constants play an important role in extracting some interesting physics quantities from diverse measurements. For example, f_B relates the measurement of the $B\bar{B}$ mixing [4] ratio to CKM matrix elements. At present it is not possible to determine f_B experimentally from the purely leptonic B decay, so theoretical calculations of f_B must be used. Hence, the calculations of f_B are of considerable importance. With the predictions for the ratios $f_{D^+} : f_{D_S^+} : f_B$, measurements of f_{D^+} and $f_{D_S^+}$ provide checks on some theoretical calculations of the decay constants and help discriminate among different models and improve the reliability of estimates of f_B .

To date, there are eight experimental measurements of $f_{D_S^+}$ from the WA75 [5], CLEO [6], BES [7], E653 [8], L3 [9], BEATRICE [10], OPAL [11] and ALEPH [12] groups. For $D^+ \rightarrow \mu^+ \nu_\mu$, the MARK-III Collaboration [13] set a branching fraction upper limit of 0.07% (corresponding to $f_{D^+} < 290$ MeV at 90% C.L.). The

BES Collaboration [14] measured $f_{D^+} = (300^{+180+80}_{-150-40})$ MeV based on one event of $D^+ \rightarrow \mu^+ \nu_\mu$ from the data collected at 4.03 GeV with the BES-I detector at the BEPC collider.

In this Letter, we report a direct measurement of the branching fraction for the decay $D^+ \rightarrow \mu^+ \nu_\mu$ and determination of the decay constant f_{D^+} .

II. THE BES-II DETECTOR

The BES-II is a conventional cylindrical magnetic detector that is described in detail in Ref. [15]. A 12-layer vertex chamber (VC) surrounding the beryllium beam pipe provides input to the event trigger, as well as coordinate information. A forty-layer main drift chamber (MDC) located just outside the VC yields precise measurements of charged particle trajectories with a solid angle coverage of 85% of 4π ; it also provides ionization energy loss (dE/dx) measurements which are used for particle identification. Momentum resolution of $1.7\% \sqrt{1 + p^2}$ (p in GeV/c) and dE/dx resolution of 8.5% for Bhabha scattering electrons are obtained for the data taken at $\sqrt{s} = 3.773$ GeV. An array of 48 scintillation counters surrounding the MDC measures the time of flight (TOF) of charged particles with a resolution of about 180 ps for electrons. Outside the TOF, a 12 radiation length, lead-gas barrel shower counter (BSC), operating in self-quenching streamer mode, measures the energies of electrons and photons over 80% of the total solid angle with an energy resolution of $\sigma_E/E = 0.22/\sqrt{E}$ (E in GeV) and spatial resolutions of $\sigma_\phi = 7.9$ mrad and $\sigma_Z = 2.3$ cm for electrons. A solenoidal magnet outside the BSC provides a 0.4 T magnetic field in the central tracking region of the detector. Three double-layer muon counters instrument the magnet flux return, and serve to identify muons of momentum greater than 500 MeV/c . They cover 68% of the total solid angle.

III. DATA ANALYSIS

The data used in the analysis were collected with the BES-II detector at the BEPC collider. A total integrated luminosity of about 33 pb^{-1} was taken at and around the center-of-mass energy of 3.773 GeV. Those are just above the threshold of $e^+e^- \rightarrow D\bar{D}$ and below the threshold of $e^+e^- \rightarrow D\bar{D}^*$. Thus, if a D^- meson decay is fully reconstructed (This is called a singly tagged D^- meson), a D^+ meson must exist in the system recoiling against the singly tagged D^- meson. From the singly tagged D^- event sample, the events of the decay $D^+ \rightarrow \mu^+ \nu_\mu$ can be well selected in the recoiling system. Therefore, the absolute branching fraction for the decay $D^+ \rightarrow \mu^+ \nu_\mu$ can be well measured and the decay constant f_{D^+} can be determined.

A. Singly tagged D^- event sample

1. Events selection

The D^- meson is reconstructed in the nine hadronic decay modes of $K^+\pi^-\pi^-$, $K^0\pi^-$, K^0K^- , $K^+K^-\pi^-$, $K^0\pi^-\pi^-\pi^+$, $K^0\pi^-\pi^0$, $K^+\pi^-\pi^-\pi^0$, $K^+\pi^+\pi^-\pi^-\pi^-$ and $\pi^+\pi^-\pi^-$. Events which contain at least three reconstructed charged tracks with good helix fits are selected. In order to ensure the well-measured 3-momentum vectors and the reliably charged particle identification, the charged tracks used in the single tag analysis are required to be within $|\cos\theta| < 0.85$, where θ is the polar angle of the charged track. All tracks, save those from K_S^0 decays, must originate from the interaction region, which require that the closest approach of the charged track in the xy plane is less than 2.0 cm and the absolute z position of the track is less than 20.0 cm. Pions and kaons are identified by means of TOF and dE/dx measurements. Pion identification requires a consistency with the pion hypothesis at a confidence level (CL_π) greater than 0.1%. In order to reduce misidentification, a kaon candidate is required to have a larger confidence level (CL_K) for a kaon hypothesis than that for a pion hypothesis. The π^0 is reconstructed in the decay of $\pi^0 \rightarrow \gamma\gamma$. To select good photons from the decay of π^0 , the energy of a photon deposited in the BSC is required to be greater than 0.07 GeV [16], and the electromagnetic shower is required to start in the first 5 readout layers. In order to reduce backgrounds, the angle between the photon and the nearest charged track is required to be greater than 22° [16] and the angle between the direction of the cluster development and the direction of the photon emission to be less than 37° [16].

For the single tag modes of $D^- \rightarrow K^+\pi^-\pi^-\pi^-\pi^-$ and $D^- \rightarrow \pi^+\pi^-\pi^-$, backgrounds are further reduced by requiring the difference between the measured energy of the D^- candidate and the beam energy to be less than 70 and 60 MeV, respectively. In addition, the cosine of the D^- production angle relative to the beam direction is required to be $|\cos\theta_{D^-}| < 0.8$.

2. Single tag analysis

For each event, there may be several different charged track (or charged and neutral track) combinations for each of the nine single tag modes. Each combination is subject to a one-constraint (1C) kinematic fit requiring overall event energy conservation and that the unmeasured recoil system has the same invariant mass as the track combinations. Candidates with a fit probability $P(\chi^2)$ greater than 0.1% are retained. If more than one combination satisfies $P(\chi^2) > 0.1\%$, the combination with the largest fit probability is retained. For the single tag modes with a neutral kaon and/or neutral pion, one additional constraint kinematic fit for the $K_S^0 \rightarrow \pi^+\pi^-$ and/or $\pi^0 \rightarrow \gamma\gamma$ hypothesis is performed, separately.

The resulting distributions in the fitted invariant masses of $mKn\pi$ ($m = 0$ or 1 or 2 and $n = 1$ or 2 or 3 or 4) combinations, which are calculated using the fitted momentum vectors from the kinematic fit, are shown in Fig. 2. The signals for the singly tagged D^- mesons are clearly observed in the fitted mass spectra. A maximum likelihood fit to the mass spectrum with a Gaussian function for the D^- signal and a special background function[19] to describe backgrounds yields the number of the singly tagged D^- events for each of the nine modes and the total number of $5321 \pm 149 \pm 160$ reconstructed D^- mesons, where the first error is statistical and the second systematic obtained by varying the parameterization of the background. The curves of Fig. 2 give the best fits to the invariant mass spectra. In the fits to the mass spectra, the standard deviations of the Gaussian signal functions for Fig. 2(g) and Fig. 2(h) are fixed at 4.27 MeV and 2.16 MeV, respectively. These standard deviations are obtained from Monte Carlo sample. All other parameters are left free in the fit.

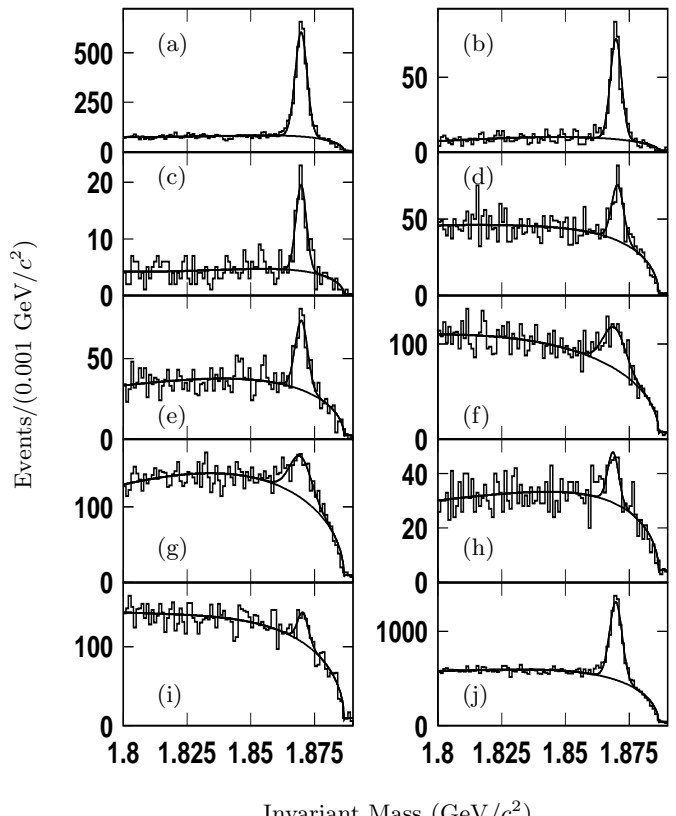


FIG. 2: The distributions of the fitted invariant masses of (a) $K^+\pi^-\pi^-$, (b) $K^0\pi^-$, (c) K^0K^- , (d) $K^+K^-\pi^-$, (e) $K^0\pi^-\pi^-\pi^+$, (f) $K^0\pi^-\pi^0$, (g) $K^+\pi^-\pi^-\pi^0$, (h) $K^+\pi^+\pi^-\pi^-\pi^-$, and (i) $\pi^-\pi^-\pi^+$ combinations; (j) the 9 modes combined together; the curves are the best fits described in the text.

B. Events of $D^+ \rightarrow \mu^+ \nu_\mu$

1. Muon Identification

To identify the muon from the decay $D^+ \rightarrow \mu^+ \nu_\mu$, the charged track in the recoil system of the D^- tag in each of the events as shown in Fig. 2 is examined for muon identification requirements. The muon identification requires:

1. The charged track satisfies $|\cos \theta| < 0.68$, where θ is the polar angle of the charged track.
2. There must be hits in the muon system and the hits must well associate with the charged track extrapolated from the track reconstructed in the MDC. The required number of the hits in the muon system is momentum dependent.
3. The muon candidate with the transverse momentum of greater than $0.7 \text{ GeV}/c$ is required to hit at least two layers of the muon system.

A charged track satisfying the 3 requirements is identified as a muon. However, a small fraction of the pions which can punch through the muon system could be misidentified as muons.

To estimate the average probability of misidentifying a pion as a muon with momentum between 0.785 and $1.135 \text{ GeV}/c$, we select the pions from the decay $J/\psi \rightarrow \omega \pi^+ \pi^-$ in the data taken at the center-of-mass energy of 3.097 GeV with the BES-II detector. The pion which satisfies $|\cos \theta_\pi| < 0.68$ (θ_π is the polar angle of the pion) and with momentum in the region from 0.785 to $1.135 \text{ GeV}/c$ is checked for whether it satisfies the muon selection requirements. A total of 10657 pions from the $J/\psi \rightarrow \omega \pi^+ \pi^-$ events satisfy the pion selection criteria and 259 of them are misidentified as muons. Those give the averaged misidentification probability of 0.024 ± 0.002 .

2. Candidates for $D^+ \rightarrow \mu^+ \nu_\mu$

Candidate events for the decay $D^+ \rightarrow \mu^+ \nu_\mu$ are selected from the surviving charged track in the system recoiling against the singly tagged D^- mesons. To select the $D^+ \rightarrow \mu^+ \nu_\mu$, it is required that there be a single charged track originating from the interaction region in the recoil system of the D^- tag and the charged track is identified as a muon with charge opposite to the charge of the tagged D^- . For the candidate event, no extra good photon which is not used in the reconstruction of the singly tagged D^- meson is allowed to be present in the event. Since there is a missing neutrino in the purely leptonic decay event, the event should be characteristic with missing energy E_{miss} and missing momentum P_{miss} which are carried by the neutrino. For the purely leptonic decay event, the reconstructed U_{miss} which is defined as

the difference between the E_{miss} and the P_{miss} should be close to zero. Fig. 3(a) shows the distribution of the U_{miss} for the Monte Carlo events of $e^+ e^- \rightarrow D^+ D^-$, where $D^- \rightarrow K^+ \pi^- \pi^-$ and $D^+ \rightarrow \mu^+ \nu_\mu$. Fig. 3(b) shows the same distribution of the U_{miss} for the Monte Carlo events of $D^- \rightarrow K^+ \pi^- \pi^- \pi^0$ and $D^+ \rightarrow \mu^+ \nu_\mu$. The distribution of the reconstructed muon momentum selected from the Monte Carlo events of $D^+ \rightarrow \mu^+ \nu_\mu$ is shown in Fig. 4, where the interval between the two dashed lines is defined as the selected muon momentum region for the events of $D^+ \rightarrow \mu^+ \nu_\mu$.

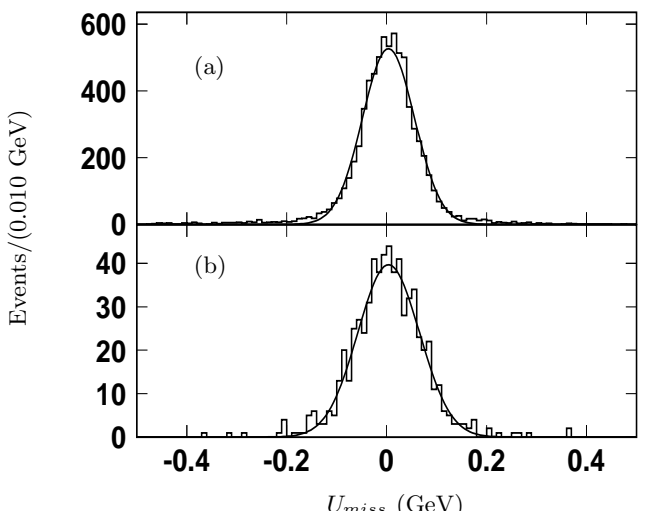


FIG. 3: The distributions of the U_{miss} calculated for the Monte Carlo events of (a) $D^+ \rightarrow \mu^+ \nu_\mu$ versus the tags of $D^- \rightarrow K^+ \pi^- \pi^-$ and (b) $D^+ \rightarrow \mu^+ \nu_\mu$ versus the tags of $D^- \rightarrow K^+ \pi^- \pi^- \pi^0$.

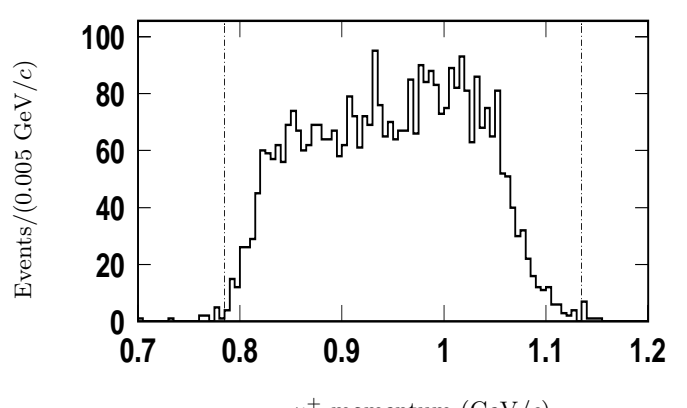


FIG. 4: The distribution of the reconstructed muon momentum selected from the Monte Carlo events of $D^+ \rightarrow \mu^+ \nu_\mu$; the interval between the two dashed lines shows the region of the selected muon momentum in the data analysis.

To select the purely leptonic decay events from the singly tagged D^- event sample, it is required that the U_{miss} of the candidate events should be within the $\pm 3\sigma_{U_{miss,i}}$ region for the single tag mode(i), where $\sigma_{U_{miss,i}}$ is the standard deviation of the $U_{miss,i}$ distribution obtained from the Monte Carlo simulation for the event of $D^+ \rightarrow \mu^+ \nu_\mu$ versus the single tag mode(i) ($i = 1$ is for $K^+ \pi^- \pi^-$; $i = 2$ is for $K^0 \pi^- \dots$ and $i = 9$ is for $\pi^+ \pi^- \pi^-$ mode). A further criterion requires that the candidate muon momentum should be in the region from 0.785 to 1.135 GeV/c as shown in Fig. 4. Fig. 5 shows the scatter-plot of the momentum of the candidate muon versus the U_{miss} , where the dots and star are for the tag modes of $K^+ \pi^- \pi^-$ and $K^+ \pi^- \pi^- \pi^0$, respectively. The solid (dashed) vertical lines give the $\pm 3\sigma_{U_{miss}}$ interval for the single tag mode of $D^- \rightarrow K^+ \pi^- \pi^-$ ($D^- \rightarrow K^+ \pi^- \pi^- \pi^0$), while the two horizontal lines give the selected momentum region for the μ^+ from the purely leptonic decays of the D^+ mesons. The regions surrounded by the lines are defined as the selected signal regions for the two single tag modes. There are 3 events within the signal regions for the two single tag modes.

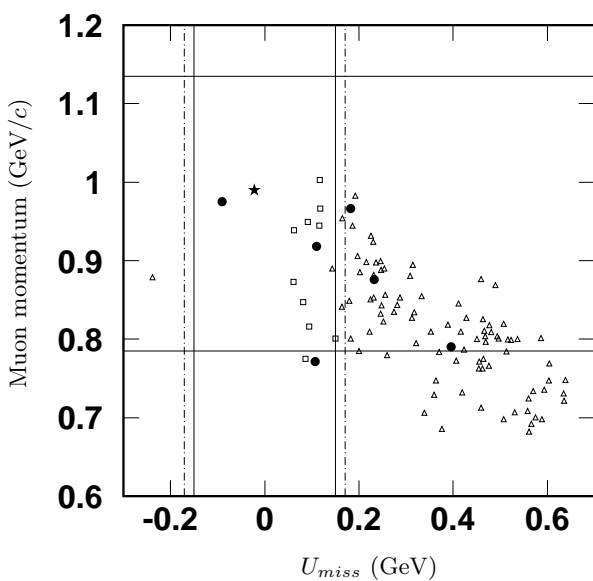


FIG. 5: The scatter-plot of the muon momentum versus U_{miss} recoiling against the muon and the single tags ($mKm\pi$ combinations) for the surviving purely leptonic decay candidates, where the dots (●) and the star (★) are for the single tag modes of $K^+ \pi^- \pi^-$ and $K^+ \pi^- \pi^- \pi^0$, respectively, those are from the data; the open squares and the open triangles are for the Monte Carlo background events from the Monte Carlo sample which is 27 times larger than the data, see text.

Fig. 6(a) shows the distribution of the fitted masses of the $mKm\pi$ combinations for the events which satisfy the selection criteria. The fitted masses of the 3 candidate events are all in the well measured D^- signal region in the

TABLE I: Three candidates for D^+ purely leptonic decay.

Event	1	2	3
Tagging mode	$K^+ \pi^- \pi^-$	$K^+ \pi^- \pi^- \pi^0$	$K^+ \pi^- \pi^-$
Fitted mass [MeV/ c^2]	1870.8	1876.9	1871.4
Number of μ layer hits	2	2	2
μ^+ momentum [GeV/ c]	0.974	0.981	0.919
U_{miss} [GeV]	-0.093	-0.023	0.117
Calculated momentum of neutrino [GeV/ c]	1.000	1.007	0.843

mass spectrum. Table I summarizes the characteristics of the 3 events. In each case, the measured mass of D^- meson, the U_{miss} of the event and the momentum of the μ^+ agree well with the expected values.

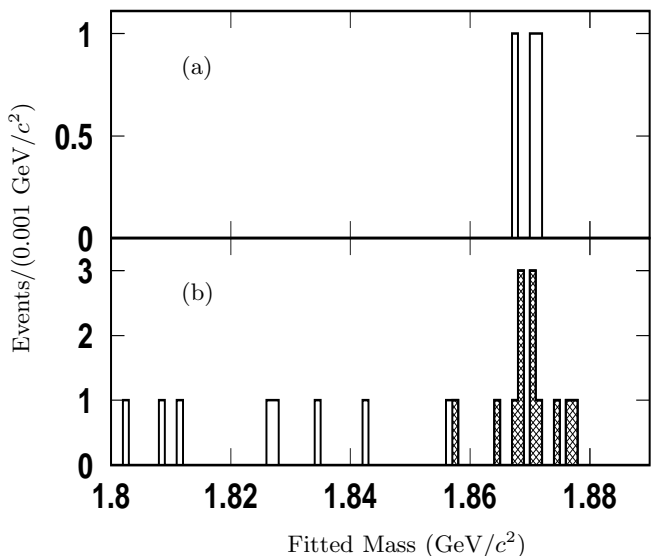


FIG. 6: The distributions of the $mKm\pi$ ($m = 0$ or 1 or 2 and $n = 1$ or 2 or 3 or 4) combinations for the events in which (a) the candidate events for $D^+ \rightarrow \mu^+ \nu_\mu$ are found in the system recoiling against the tags ($mKm\pi$ combinations) and (b) only one charged track is found in the system recoiling against the tags and the events satisfy the kinematic requirements for selecting the purely leptonic decay events, but these events do not satisfy muon identification requirements.

3. Background subtraction

Some non-purely leptonic events from the D^+ decays may also satisfy the selection criteria and are the background to the purely leptonic decay events. These back-

ground events must be subtracted. The number of the background events is estimated by analyzing the Monte Carlo sample which is 27 times larger than the data. The Monte Carlo events are generated as $e^+e^- \rightarrow D\bar{D}$ and the D and \bar{D} mesons are set to decay to all possible final states according to the decay modes and the branching fractions quoted from PDG [2] except the purely leptonic decay mode under study. In Fig. 5, the open squares (\square) and the open triangles (\triangle) are for the background events from the Monte Carlo sample, where the \square and the \triangle indicate that the background events are within and outside of the $\pm 3\sigma_{U_{miss,i}}$ interval, respectively. There are 9 background events satisfying the selection criteria in the signal regions. This number of the background events is then normalized to the corresponding data set. A total of 0.33 ± 0.11 background events are estimated in the 3 candidates for $D^+ \rightarrow \mu^+\nu_\mu$. After subtracting this number of the background events, 2.67 ± 1.74 signal events for $D^+ \rightarrow \mu^+\nu_\mu$ decay are retained.

The number of the background events can also be estimated from the number of the singly tagged D^- events in which only one charged track in the recoiling system is found and the charged track is not identified as a muon. Fig. 6(b) shows the distribution of the fitted masses of the $mKn\pi$ combinations from the events. These events satisfy the kinematic requirements for selecting the purely leptonic decay events, but the charged track in the recoiling system do not satisfy the muon identification requirements. There are 13 events in the D^- signal regions as shown in the hatched histogram. The average probability of misidentifying a pion as a muon discussed previously yields the number of the background events in the 3 purely leptonic decay candidates to be 0.31 ± 0.09 , which is consistent with 0.33 ± 0.11 estimated from the Monte Carlo sample[20].

IV. RESULT

A. Monte Carlo Efficiency

The efficiency for reconstruction of the purely leptonic decay $D^+ \rightarrow \mu^+\nu_\mu$ after tagging the D^- meson is estimated by Monte Carlo simulation. A Monte Carlo study gives that the efficiency is $\epsilon_{\mu^+\nu_\mu} = (41.7 \pm 1.1)\%$.

B. Branching fraction

To determine the purely leptonic decay branching fraction and the decay constant based on the observed numbers of the purely leptonic decay events and the singly tagged D^- mesons, we build a likelihood function L , which is the product of the Poissonian probability function for observation of the purely leptonic decay events and the Gaussian function for the number of the singly tagged D^- mesons. Let $N_{\mu^+\nu_\mu}$ be the number of the observed purely leptonic decay events ($N_{\mu^+\nu_\mu} = 3.0$,

N_{tag} be the number of the singly tagged D^- mesons ($N_{tag} = 5321 \pm 149 \pm 160$), $n_{\mu^+\nu_\mu}$ and n_{tag} be the corresponding expected numbers of the events, respectively. The likelihood function is then given by

$$L = P(n_{\mu^+\nu_\mu}, N_{\mu^+\nu_\mu})G(n_{tag}, N_{tag}), \quad (2)$$

with abbreviation

$$P(n_{\mu^+\nu_\mu}, N_{\mu^+\nu_\mu}) = \frac{(n_{\mu^+\nu_\mu})^{N_{\mu^+\nu_\mu}}}{N_{\mu^+\nu_\mu}!} e^{-n_{\mu^+\nu_\mu}}$$

and

$$G(n_{tag}, N_{tag}) = \frac{1}{\sqrt{2\pi\sigma_{N_{tag}}}} e^{-\frac{(N_{tag}-n_{tag})^2}{2\sigma_{N_{tag}}^2}}, \quad (3)$$

where the $\sigma_{N_{tag}}$ is the systematic uncertainty in the number of the singly tagged D^- mesons ($\sigma_{N_{tag}} = 160$).

For the observed numbers of the purely leptonic decay events and the singly tagged D^- mesons, the expected number of the purely leptonic decay events is given by

$$n_{\mu^+\nu_\mu} = n_{tag}BF\epsilon_{\mu^+\nu_\mu} + n_b, \quad (4)$$

where BF is the purely leptonic decay branching fraction and n_b is the number of the background events. The value of the likelihood function is obtained by integrating over $N_{\mu^+\nu_\mu}$,

$$L(BF) = \int L(BF, N_{\mu^+\nu_\mu})dN_{\mu^+\nu_\mu}, \quad (5)$$

which is shown as a function of BF in Fig. 7. The maximum likelihood occurs at $BF = 0.122\%$. Integrating the function from the maximum position to -1σ ($+1\sigma$) value corresponding to 68.3% of the total area below (above) the peak position yields the statistical error to be -0.053% ($+0.111\%$). The relative systematic uncertainty arises mainly from the uncertainties in the μ^+ identification ($\pm 5.0\%$), tracking efficiency ($\pm 2.0\%$), background subtraction ($\pm 5.6\%$) and U_{miss} cut ($\pm 1.0\%$). Adding these uncertainties in quadrature gives the total relative systematic uncertainty to be $\pm 7.8\%$. Finally, we obtain

$$BF(D^+ \rightarrow \mu^+\nu_\mu) = (0.122^{+0.111}_{-0.053} \pm 0.010)\%.$$

C. Decay constant f_{D^+}

The decay constant f_{D^+} can be obtained by inserting the mass of the muon, the mass of the D^+ meson, the CKM matrix element $|V_{cd}|$, the Fermi coupling constant G_F and the lifetime of the D^+ meson [2] into equation (1). By substituting $BF(D^+ \rightarrow \mu^+\nu_\mu)$ in terms of f_{D^+}

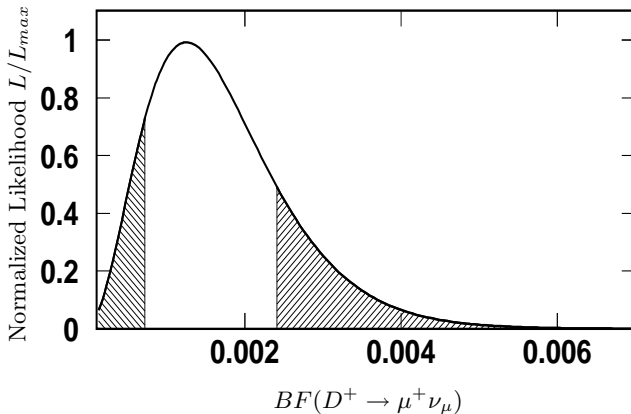


FIG. 7: The dependence of the normalized likelihood on the branching fraction for the decay of $D^+ \rightarrow \mu^+\nu_\mu$.

into equation (5), we obtain the relation of the likelihood function with f_{D^+} ,

$$L(f_{D^+}) = \int L(f_{D^+}, N_{\mu^+\nu_\mu}) dN_{\mu^+\nu_\mu}. \quad (6)$$

The most probable value of f_{D^+} and its statistical error can be obtained by integrating over $N_{\mu^+\nu_\mu}$. The dependence of the likelihood function on the decay constant f_{D^+} is shown in Fig. 8. Following the procedure for extracting the $BF(D^+ \rightarrow \mu^+\nu_\mu)$, we finally obtain

$$f_{D^+} = (371_{-119}^{+129} \pm 25) \text{ MeV},$$

where the first error is statistical and the second systematic which arises mainly from the uncertainties in the measured branching fraction ($\pm 4.1\%$), the CKM matrix element $|V_{cd}|$ ($\pm 5.4\%$), and the lifetime of the D^+ meson ($\pm 0.3\%$) [2]. These uncertainties are added in quadrature to obtain the total systematic error, which is $\pm 6.8\%$.

V. SUMMARY

From the $5321 \pm 149 \pm 160$ singly tagged D^- mesons, 2.67 ± 1.74 purely leptonic decay events of $D^+ \rightarrow \mu^+\nu_\mu$

are observed in the system recoiling against the singly tagged D^- mesons, resulting in the branching fraction of $BF(D^+ \rightarrow \mu^+\nu_\mu) = (0.122_{-0.053}^{+0.111} \pm 0.010)\%$ and the decay constant of $f_{D^+} = (371_{-119}^{+129} \pm 25)$ MeV. The measured values are independent of the D^+D^- cross section and luminosity. They do not require model-dependent assumptions. Thus, they are absolute measurements. The central value of f_{D^+} is consistent with that measured using the BES-I detector [14]. The measured value of f_{D^+} is also consistent with most theoretical predictions, which are in the range from 90 to 360 MeV [3].

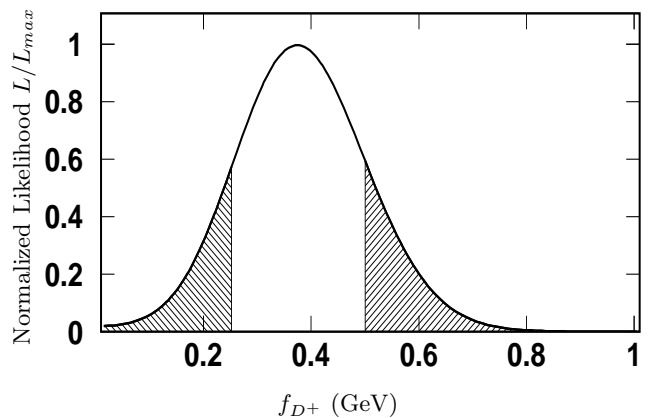


FIG. 8: The dependence of the normalized likelihood on the decay constant f_{D^+} .

ACKNOWLEDGEMENTS

The BES Collaboration thanks the staff of BEPC for their hard efforts. This work is supported in part by the National Natural Science Foundation of China under contracts Nos. 19991480, 10225524, 10225525, the Chinese Academy of Sciences under contract No. KJ 95T-03, the 100 Talents Program of CAS under Contract Nos. U-11, U-24, U-25, and the Knowledge Innovation Project of CAS under Contract Nos. U-602, U-34(IHEP); by the National Natural Science Foundation of China under Contract No.10175060(USTC), and No.10225522(Tsinghua University).

[1] D. Silverman, H. Yao, Phys. Rev. D **38** (1988) 214; J.L. Rosner, Phys. Rev. D **42** (1990) 3732; C.H. Chang, Y.Q. Chen, Phys. Rev. D **46** (1992) 3845; Phys. Rev. D **49** (1994) 3399.
[2] S. Eidelman, et al., Particle Data Group, Phys. Lett. B **592** (2004) 1.
[3] M. Suzuki, Phys. Lett. B **162** (1985) 392; S.N. Sinha,

Phys. Lett. B **178** (1986) 110; D. Silverman, H. Yao, Phys. Rev. D **38** (1988) 214; S. Capstick, S. Godfrey, Phys. Rev. D **41** (1990) 2856.
[4] C. Bernard, et al., arXiv:hep-ph/9709328; C.O. Dib, et al., Phys. Rev. D **41** (1990) 1522; S. Capstick and S. Godfrey, Phys. Rev. D **41** (1990) 2856; M. Wetherell, Charm Weak Decay, in: Proceedings of XVI International Sym-

posium on Photon-Lepton Physics, Cornell University, Ithaca, New York, August, 1993.

[5] S. Aoki, et al., WA75 Collaboration, *Progress of Theor. Phys.* **89** (1993) 131.

[6] D. Acosta, et al., CLEO Collaboration, *Phys. Rev. D* **49** (1994) 5690; M. Chada, et al., CLEO Collaboration, *Phys. Rev. D* **49** (1998) 032002.

[7] J.Z. Bai, et al., BES Collaboration, *Phys. Rev. Lett.* **74** (1995) 4599.

[8] K. Kodama, et al., E653 Collaboration, *Phys. Lett. B* **382** (1996) 299.

[9] M. Acciarri, et al., L3 Collaboration, *Phys. Lett. B* **396** (1997) 327.

[10] Y. Alexandrov, et al., BEATRICE Collaboration, *Phys. Lett. B* **478** (2000) 31.

[11] G. Abbiendi, et al., OPAL Collaboration, *Phys. Lett. B* **516** (2001) 236.

[12] A. Heister, et al., ALEPH Collaboration, *Phys. Lett. B* **528** (2002) 1.

[13] J. Adler, et al., MARK-III Collaboration, *Phys. Rev. Lett.* **60** (1998) 1375.

[14] J.Z. Bai, et al., BES Collaboration, *Phys. Lett. B* **429** (1998) 188.

[15] J.Z. Bai, et al., BES Collaboration, *Nucl. Instr. Meth. A* **458**, 627 (2001).

[16] M. Ablikim, et al., BES Collaboration, *Phys. Lett. B* **597** (2004) 39, arXiv:hep-ex/0406028

[17] Ian C. Brock, Mn-Fit, a fitting and plotting package using MINUIT, Version 4.07, December 22, 2000.

[18] G. Bonvicini, et al. CLEO Collaboration, *Phys. Rev. D* **70** (2004) 112004, arXiv:hep-ex/0411050.

[19] A Gaussian function was assumed for the signal. The background shape was

$$(1.0 + p_1 y + p_2 y^2) N \sqrt{1 - (\frac{x}{E_b})^2} x e^{-f(1 - \frac{x}{E_b})^2} + c,$$

where $N \sqrt{1 - (\frac{x}{E_b})^2} x e^{-f(1 - \frac{x}{E_b})^2}$ is the ARGUS background shape, x is the fitted mass, E_b is the beam energy, $y = (E_b - x)/(E_b - 1.8)$, N , f , p_1 , p_2 and c are the fit parameters. The parameter c accounts for the varying of the beam energy. The ARGUS background shape was used by the ARGUS experiment to parameterize the background for fitting B mass peaks. For details, see [17].

[20] In response to the comment of the paper [18], we here describe the background estimation in more detail. We estimated the number of background events using two different methods. In the first method, we estimated the number of background events using the Monte Carlo events of $e^+e^- \rightarrow D\bar{D}$. The Monte Carlo sample of $D\bar{D}$ production and decays are generated as $e^+e^- \rightarrow D^0\bar{D}^0, D^+D^-$, where the ratio of the neutral over the total $D\bar{D}$ production cross section is set to be 0.58. Both D and \bar{D} mesons decay to all possible modes (which of course include $D^+ \rightarrow \pi^+\pi^0, \bar{K}^0\pi^+$, ...) according to the branching fractions quoted from PDG [2]. The decay channel $D^+ \rightarrow \tau^+\nu$ which is not currently listed in the PDG was added into the Monte Carlo sample to estimate the number of background events. The branching fraction for $D^+ \rightarrow \tau^+\nu$ is estimated based on assuming decay constant $f_{D^+} = 220$ MeV. In the second method, we use the data (see Fig. 6) to estimate the number of background events. The number of background events obtained from the data include all possible contribution from other D decay channels as well as the possible continuum backgrounds.